Zerumbone from *Zingiber zerumbet* Ameliorates Lipopolysaccharide-Induced ICAM-1 and Cytokines Expression *via* p38 MAPK/JNK-IκB/NF-κB Pathway in Mouse Model of Acute Lung Injury

Chien-Ying Lee[1, 2], Shih-Pin Chen[3, 4], Chun-Hung Su[3, 4], Yung-Chyuan Ho[5],
Ming-Ling Yang[6], Shiuan-Shinn Lee[7], Rosa Huang-Liu[8], Ching-Ping Yang[9],
Chun-Jung Chen[9], and Yu-Hsiang Kuan[1, 2]

[1]*Department of Pharmacology, School of Medicine, Chung Shan Medical University, Taichung 40201*
[2]*Department of Pharmacy, Chung Shan Medical University Hospital, Taichung 40201*
[3]*Department of Internal Medicine, School of Medicine, Chung Shan Medical University,
Taichung 40201*
[4]*Department of Internal Medicine, Chung Shan Medical University Hospital, Taichung 40201*
[5]*School of Medical Applied Chemistry, Chung Shan Medical University, Taichung 40201*
[6]*Department of Anatomy, School of Medicine, Chung Shan Medical University, Taichung 40201*
[7]*School of Public Health, Chung Shan Medical University, Taichung 40201*
[8]*School of Nutrition, Chung Shan Medical University, Taichung 40201*
and
[9]*Department of Education and Research, Taichung Veterans General Hospital, Taichung 40705,
Taiwan, Republic of China*

Abstract

Acute lung injury (ALI) is a clinical syndrome with high morbidity and mortality rates mainly caused by Gram-negative bacteria. Nevertheless, an effective treatment strategy for ALI is yet to be developed. Zerumbone, a sesquiterpene isolated from *Zingiber zerumbet* Smith, possesses several advantageous bioeffects such as antioxidation, anti-inflammation, and antiulcer. Pretreatment of zerumbone inhibited lipopolysaccharide (LPS)-induced arterial blood gas exchange, neutrophils infiltration, and increased pulmonary vascular permeability. LPS-induced expression of intercellular adhesion molecule-1 (ICAM-1) was inhibited by zerumbone at a lower concentration than that of vascular cell adhesion molecule-1 (VCAM-1). In addition, proinflammatory cytokines, such as interleukin (IL)-1β and macrophage inflammatory protein (MIP)-2 were suppressed by zerumbone. The phosphorylation of nuclear factor (NF)-κB, a proinflammatory transcription factor, and degradation of inhibitor of κB (IκB), an inhibitor of NF-κB, were also reduced by zerumbone. Furthermore, we found the inhibitory concentration of zerumbone on phosphorylation of p38 mitogen-activated protein kinase (MAPK) and c-Jun NH2-terminal kinase (JNK) was lower than that of extracellular signal-regulated kinase (ERK). In conclusion, zerumbone could be a potential protective agent for ALI, possibly via expression of ICAM-1, IL-1β, and MIP-2. The protective mechanism of zerumbone was by reversing the activation of p38 MAPK/JNK-IκB/NF-κB pathway.

Key Words: acute lung injury, ICAM-1, MAPK, NF-κB, zerumbone

Introduction

Zerumbone is the major component of the essential oil extracted from *Zingiber zerumbet* rhizome (15). *Zingiber zerumbet*, known locally in tropical and subtropical areas mainly in Southeast Asia, is a traditional or alternative medicine and has been reported to possess antioxidation, anti-inflammation, antiulcer, antitumor, antinociception, antihypersension, antibacterial, antihyperglycemia, and antiplatelet activities (2, 14, 22, 38). Zerumbone is usually used as a condiment for flavoring food and also for medicinal applications to act against oxidation, inflammation, tumor formation, bacterial infection, and mutagenic and microbial activities (1, 24, 25, 28, 30). Our previous report shows that zerumbone reduces the occurrence of lipopolysaccharide (LPS)-induced acute lung injury (ALI) *via* antioxidative enzymes and Nrf2/HO-1 pathway (18). There is no information at present concerning the effect of zerumbone on the expression of adhesion molecules, cytokines, mitogen-activated protein kinase (MAPK) and nuclear factor (NF)-κB activation in LPS-induced ALI in *in vivo* assay.

Owing to its specific physiological characteristics including hypoxemia and neutrophils infiltration, the lung is susceptible to many risk factors such as infections, transfusion, aspiration, sepsis, and trauma (12). The incidence of ALI is depending on various factors and ranges from 1.5 to 78.9 per 100,000 person-years (23). According to community-based survey in clinical trial, the mortality of ALI today is still as high as 35-40% (35). Excessive expression of proinflammatory cytokines including interleukin (IL)-1β and macrophage inflammatory protein (MIP)-2, and adhesion molecules such as intercellular adhesion molecule-1 (ICAM-1) and vascular cell adhesion molecule-1 (VCAM-1), induced by risk factors results in pulmonary inflammatory disease called ALI or its severe form, the acute respiratory distress syndrome (ARDS) (13). NF-κB, an important transcription factor, is a mediator in the expression of proinflammatory cytokines and adhesion molecules which contributes abundantly in the regulation of inflammation and oxidative stress in ALI (21, 32). In addition, MAPK family, including extracellular signal-regulated kinase (ERK) 1/2, p38 MAPK, and c-Jun NH2-terminal kinase (JNK), has been demonstrated to play a critical role in NF-κB activation and pro-inflammatory gene expression in mice with LPS-induced ALI (5). At present study, we sought to investigate the protective effects of zerumbone *via* MAPK family and NF-κB activation in mice with LPS-induced ALI.

Materials and Methods

Materials

Enzyme-linked immunosorbent assay (ELISA) kits for ICAM-1, VCAM-1, MIP-2, and interleukin 1 beta (IL-1β) were obtained from R&D Systems (Minneapolis, MN, USA). Antibodies against inhibitor of κB (IκB), β-actin, and phosphorylated and non-phosphorylated forms of p65, p38, JNK, and ERK were purchased from Santa Cruz Biotechnology (Santa Cruz, CA, USA). Secondary antibodies were obtained from Jackson Immuno Research Laboratories (Baltimore, MD, USA). Protein markers were obtained from Biotools Co. Ltd. (Taiwan). Tissue Protein Extraction Reagent (T-PER) solution was purchased from Pierce Biotechnology (Rockford, Ill, USA). LPS from *Escherichia coli* Serotype 0111:B4, zerumbone, and other reagents, unless specifically stated elsewhere, were purchased from Sigma-Aldrich (St. Louis, MO, USA).

Animals

Adult male pathogen-free ICR mice weighting 25-30 g were purchased from BioLASCO (Taipei, Taiwan). All animals were fed the standard laboratory diet and water *ad libitum*. The mice were kept at a temperature of 22 ± 1°C under a relative humidity of 50-60% with 12 h light-dark cycle. All experimental protocols and care of mice were approved by the Institutional Animal Care and Use Committee of Chung Shan Medical University.

Experimental Design of LPS-Induced ALI in Murine Model

The murine model of LPS-induced ALI was performed as described in previous study (37). Briefly, the mice were randomly divided into six groups including a control group and five treatment groups. The control group was challenged by intraperitoneal (i.p.) administration of solvent for 30 min before received 50 μl of saline for 6 h *via* intratracheal (i.t.) administration. The five treatment groups were pretreated with various concentrations of zerumbone at 0, 21.8, 218.3, and 2183.4 μg/kg or dexamethasone at 1 mg/kg respectively for 30 min, followed by i.t. administration of LPS at 4 mg/kg for 6 h. Finally, all mice were euthanized by chloral hydrate overdose and samples were collected.

Blood Gas Analysis of Arterial Blood

After animals were sacrificed, blood samples from the abdominal aorta were collected for mea-

surement of blood gas. The partial pressures of oxygen (pO_2), partial pressures of carbon dioxide (pCO_2), and blood acidity (pH) were detected by blood gas analyzer (Radiometer ABL 700 blood gas analyzer, Copenhagen, Denmark).

Bronchoalveolar Lavage Fluid (BALF) Collection and Protein Concentration Assay

After euthanization, the lavage of lung was performed gently using 1 ml of sterile saline *via* a tracheal cannula for three times. Lavage fluids from all three rounds were collected and pooled together before centrifuged at 600 g for 10 min at 4°C. The resulting supernatant was stored at -20°C for subsequent protein concentration, cytokines generation, and adhesion molecules expression assays. In addition, the sediment cell pellets were gently centrifuged onto glass slides by cytospinning and subjected to Wright-Giemsa stain. Neutrophil count was determined according to nuclear morphology (4).

Measurement of Protein Concentration, Cytokines, and Adhesion Molecules Expression

Total protein concentration in cell-free BALF supernatant was measured using the Bradford protein assay. Generation of cytokines, including MIP-2 and IL-1β, and expression of adhesion molecules, such as ICAM-1 and VCAM-1, were measured by commercially available ELISA assay kits. The quantification of protein, cytokines, and adhesion molecules was performed according to the manufacturer's instructions (11).

Measurement of mRNA Expression of Cytokines and Adhesion Molecules

Total cellular RNA of ICAM-1, VCAM-1, MIP-2, and IL-1β was extracted from lung tissue with TRIzol reagent. After addition of 1-bromo-3-chloropropane reagent, the sample was vortexed and then separated by centrifugation at 12,000 g for 15 min at 4°C. The total RNA was precipitated with isopropanol at 12,000 g for 10 min at 4°C. To measure the synthesis of cDNA from total RNA, High-Capacity cDNA Reverse Transcription Kit was used. Primers were designed using the PrimerExpress 2.0 software (Applied Biosystems). The sequence of primers used was as follows: forward primer TACGTGT-GCCATGCCTTTAGC and reverse primer GC-CCACAATGACCAGCAGTA for ICAM-1; forward primer TCTCTCAGGAAATGCCACCC and reverse primer CACAGCCAATAGCAGCACAC for VCAM-1; forward primer CTCTCAAGGGCGGTCAAAAAGTT

and reverse primer TCAGACAGCGAGGCA-CATCAGGTA for MIP-2; and forward primer TCCAGGATGAGGACATGAGCAC and reverse primer GAACGTCACACACCAGCAGGTTA for IL-1β. Real-time quantitative polymerase chain reaction (PCR) analysis was performed to detect specific gene expression in FastStart Universal SYBR Green Master, primers, and cDNA samples. For the real-time quantitative DNA PCR analysis, Applied Biosystems 48-well StepOne™ Real Time PCR System was used.

Western Blot Assay for Protein Analysis

As previously described (11), lung tissues were harvested and homogenized in T-PER tissue protein extraction solution containing 1% proteinase inhibitor cocktail and phosphatase inhibitor cocktail. After centrifugation, protein samples from supernatant were collected for further analysis. Western blot was performed after sodium dodecyl sulfate polyacrylamide gel electrophoresis (SDS-PAGE) separation of proteins on the SDS gel and transfer to polyvinylidene difluoride membranes. The membranes were blocked with 5% non-fat milk (w/v) in phosphate buffer saline containing 0.1% Tween-20. After washing, the membranes were blotted with antibodies including IκB, β-actin, and phosphorylated and non-phosphorylated forms of p65, p38, JNK, and ERK. The membranes were washed again, then a 1:10,000 (v/v) dilution of horseradish peroxidase-labeled IgG was added and the blots were developed using enhanced chemiluminescence (ECL) western blotting reagents.

Statistical Analysis

All data were expressed as mean ± standard deviation (SD). Primary statistical analyses were performed by analysis of variance (ANOVA) followed by the Bonferroni's test for multi-group comparisons; $P < 0.05$ was considered significant for all tests. At least four independent experiments were performed as indicated in detail in figure legends.

Results

Effect of Zerumbone on Arterial Blood Gas in LPS-Induced ALI

To study the effects of zerumbone on LPS-induced ALI, the mice were pretreated with zerumbone for 30 min before LPS administration. As shown in Fig. 1, pH and PaO_2 were significantly decreased while $PaCO_2$ was significantly increased in the LPS-treated groups. However, the effects were
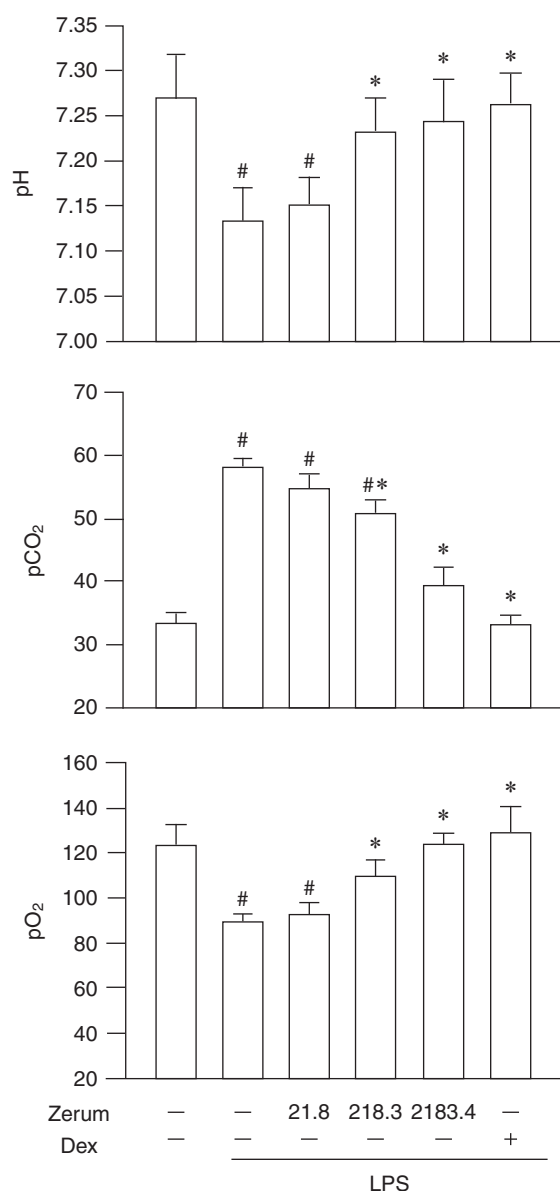
Fig. 1. Effects of zerumbone on change of arterial blood gas in LPS-induced ALI. The represented parameters are PaO_2, $PaCO_2$, and pH. Values are expressed as mean $\pm$ SD of 4 mice per group. # represents a significant difference between the indicated and normal control group, and * represents a significant difference between the indicated and LPS treated groups, $P < 0.05$.
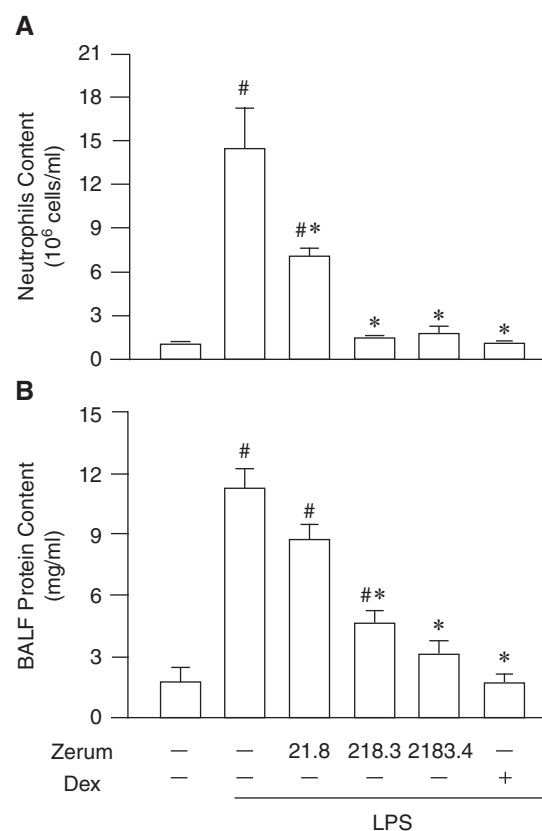

Fig. 2. Effects of zerumbone on LPS-induced neutrophils infiltration and protein leakage in BALF. (A) Neutrophils infiltration determined by Wright-Giemsa stain; (B) protein leakage determined by Bradford protein assay. Values are expressed as mean $\pm$ SD (n = 3 in each group). # represents a significant difference between the indicated and normal control group, and * represents a significant difference between the indicated and LPS treated groups, $P < 0.05$.

reversed by dexamethasone. Moreover, these effects were attenuated by zerumbone in a concentration-dependent manner, significant inhibitory effect was observed to begin at 218.3 µg/kg ($P < 0.05$).

Effect of Zerumbone on LPS-Induced Neutrophils Infiltration and Protein Leakage in BALF

Neutrophils infiltration plays an important role in the inflammatory response which characterizes ALI (4). Extensive neutrophils infiltration into alveolar space was induced after treated with LPS for 6 h. LPS-induced neutrophils infiltration was significantly inhibited by dexamethasone (Fig. 2A). Pretreatment with zerumbone suppressed neutrophils influx into alveolar space induced by LPS in a concentration-dependent manner, significant differences were observed starting from treated with 218.3 µg/kg of zerumbone and up ($P < 0.05$, Fig. 2A). LPS-induced neutrophils infiltration was caused by the increased permeability in pulmonary vascular barrier. Protein level in BALF, an indicator of permeability in pulmonary vascular barrier, was significantly up-regulated in the LPS-treated mice. LPS-induced protein leakage was significantly inhibited by dexamethasone (Fig. 2B). Pretreatment with zerumbone suppressed protein leakage into BALF in a concentration-dependent manner, significant
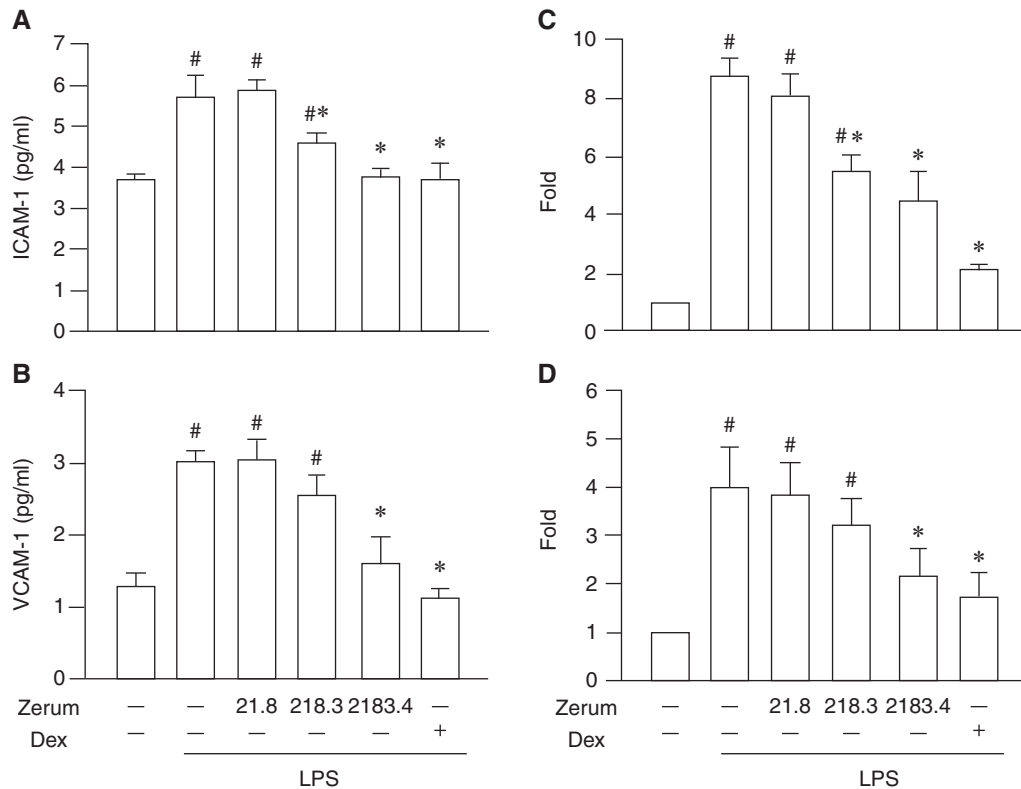
Fig. 3. Effect of zerumbone on LPS-induced expression of adhesion molecules ICAM-1 and VCAM-1. Exchanges in protein expression were shown for ICAM-1 (A) and VCAM-1 (B) in BALF. Fold-changes in mRNA expression were shown for ICAM-1 (C) and VCAM-1 (D) in lungs. Values are expressed as mean ± SD (n = 3 in each group). # represents a significant difference between the indicated and normal control group, and * represents a significant difference between the indicated and LPS treated groups, $P < 0.05$.

differences were observed starting from 218.3 μg/kg of zerumbone and up ($P < 0.05$, Fig. 2B).

Effect of Zerumbone on LPS-Induced Adhesion Molecules Expression in BALF

Adhesion molecules ICAM-1 and VCAM-1 play important roles in neutrophils infiltration into alveolar space (37). At present, we found that the expression of adhesion molecules ICAM-1 and VCAM-1, protein in BALF, and mRNA in the lungs were raised significantly in the LPS-induced ALI groups as compared with control group ($P < 0.05$). LPS-induced expression of ICAM-1 and VCAM-1 was significantly inhibited by dexamethasone (Fig. 3). Pretreatment with zerumbone suppressed LPS-induced ICAM-1 expression in a concentration-dependent manner, significant effect starting at 218.3 μg/kg ($P < 0.05$). However, significant inhibition on the VCAM-1 expression was not observed until the concentration of zerumbone was up to 2183.4 μg/kg ($P < 0.05$).

Effect of Zerumbone on LPS-Induced Cytokines

Generation in BALF

Cytokines such as MIP-2 and IL-1β are critical proinflammatory mediators in the recruitment of peripheral neutrophils into alveolar space and in the meanwhile increase the expression of adhesion molecules (36). Generation of cytokines MIP-2 and IL-1β, protein in BALF, and mRNA in the lungs were increased significantly in the LPS-administered groups as compared with control group. LPS-induced generation of MIP-2 and IL-1β was significantly inhibited by dexamethasone (Fig. 4). Pretreatment with zerumbone reduced LPS-induced expression of MIP-2 and IL-1β in a concentration-dependent manner, significant effect starting at 218.3 μg/kg ($P < 0.05$, Fig. 4).

Effect of Zerumbone on LPS-Induced IκB Degradation and p65 Phosphorylation in Lung

IκB-NF-κB pathway participates in adhesion molecules expression and cytokines generation in LPS-induced ALI (16). After LPS treatment, IκB was significantly degraded in lung tissues
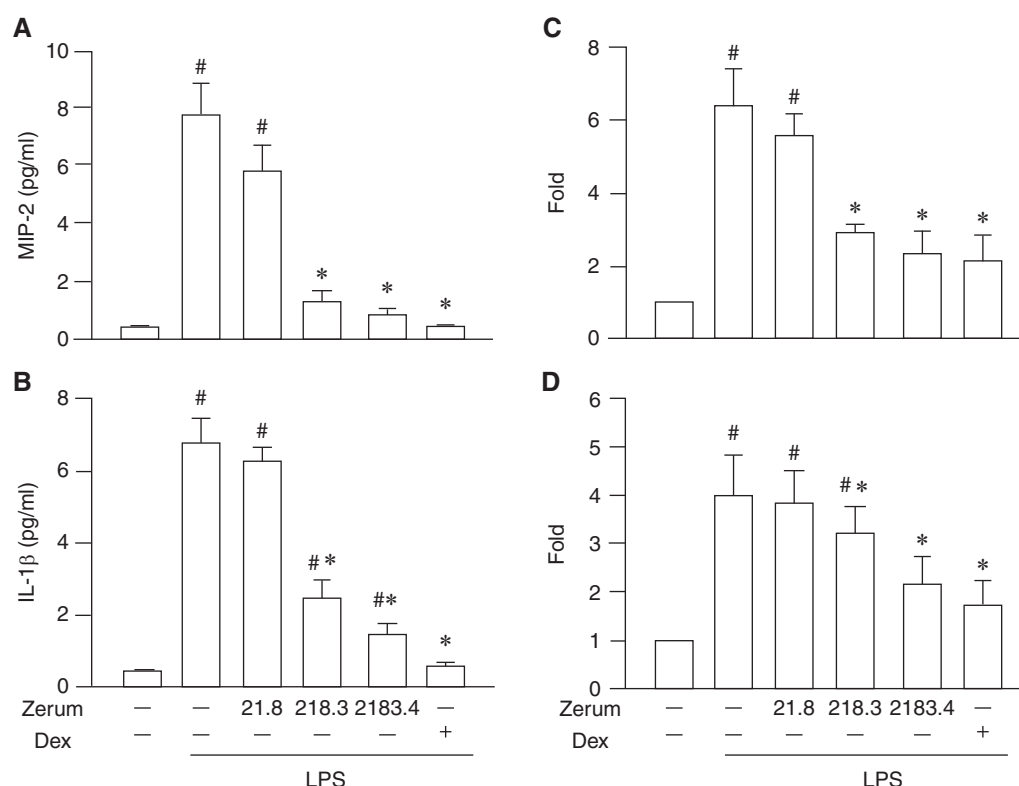
Fig. 4. Effect of zerumbone on expression of LPS-induced cytokines MIP-2 and IL-1β. Exchanges in protein expression were shown for MIP-2 (A) and IL-1β (B) in BALF. Fold-changes in mRNA expression were shown for MIP-2 (C) and IL-1β (D) in lungs. Values are expressed as mean ± SD (n = 3 in each group). # represents a significant difference between the indicated and normal control group, and * represents a significant difference between the indicated and LPS treated groups, $P < 0.05$.

in comparison with the control group ($P < 0.05$). LPS-induced IκB degradation was significantly inhibited by dexamethasone (Fig. 5). Pretreatment with zerumbone suppressed IκB degradation in a concentration-dependent manner, significant effect starting at 218.3 μg/kg ($P < 0.05$, Fig. 5). In addition, we also found that p65 phosphorylation was significantly expressed in lung tissues in LPS-treated groups when compared with the control group ($P < 0.05$). LPS-induced p65 phosphorylation was significantly inhibited by dexamethasone (Fig. 5). Pretreatment with zerumbone suppressed the phosphorylation of NF-κB in a concentration-dependent manner, significant effect also starting at 218.3 μg/kg ($P < 0.05$, Fig. 5).

Effect of Zerumbone on LPS-Induced Phosphorylation of MAPK Family in Lung

MAPK family, which contains p38 MAPK, JNK, and ERK, has been shown as the upstream factor in activation of IκB-NF-κB pathway in LPS-induced ALI (33). LPS significantly induced the phosphorylation of p38 MAPK, JNK, and ERK

when compared with the control group. LPS-induced phosphorylation of MAPK was significantly inhibited by dexamethasone (Fig. 6). LPS-induced phosphorylation of p38 MAPK and JNK was inhibited by zerumbone in a concentration-dependent manner, significant effect starting at 21.83 μg/kg ($P < 0.05$, Fig. 6). However, significant inhibition on the phosphorylation of ERK was not observed until the concentration of zerumbone was up to 2183.4 μg/kg ($P < 0.05$, Fig. 6).

Discussion

ALI is an inflammatory lung disease which is life-threatening for seriously ill patients and a frequent complication of sepsis caused by many risk factors (9). Gram negative bacterial infection is the major risk factor for ALI *via* sepsis and pneumonia. LPS is a lipid based carbohydrate polymer and the major component in the outer surface membrane of Gram negative bacteria (26). Hypoxemia, which means the low level of oxygen in arterial blood, is one of the important characteristics for ALI. Bilateral pulmonary neutrophils infiltration can lead to diminishing lung
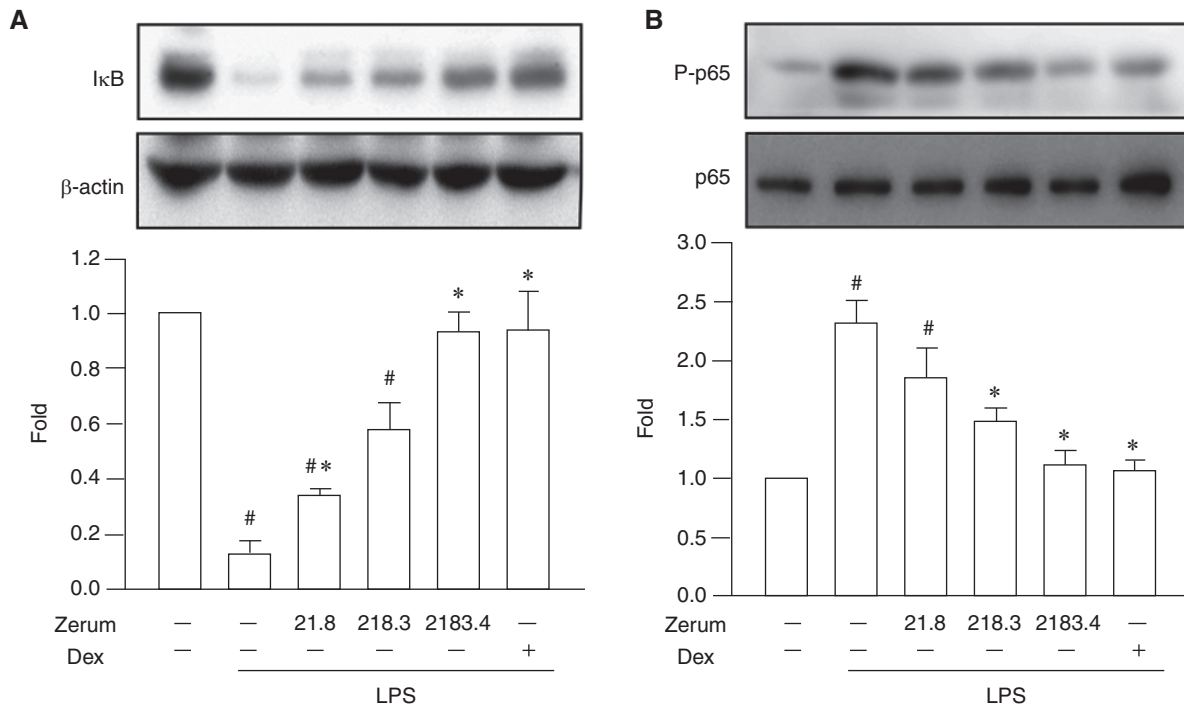
Fig. 5. Effect of zerumbone on LPS-induced IκB degradation (A) and p65 phosphorylation (B) in lungs. Lung tissues harvested from post-treated mice were analyzed by Western blotting. The fold of IκB degradation and p65 phosphorylation between the treated and control groups were calculated. Values are expressed as mean ± SD (n = 3 in each group). # represents a significant difference between the indicated and normal control group, and * represents a significant difference between the indicated and LPS treated groups, $P < 0.05$.
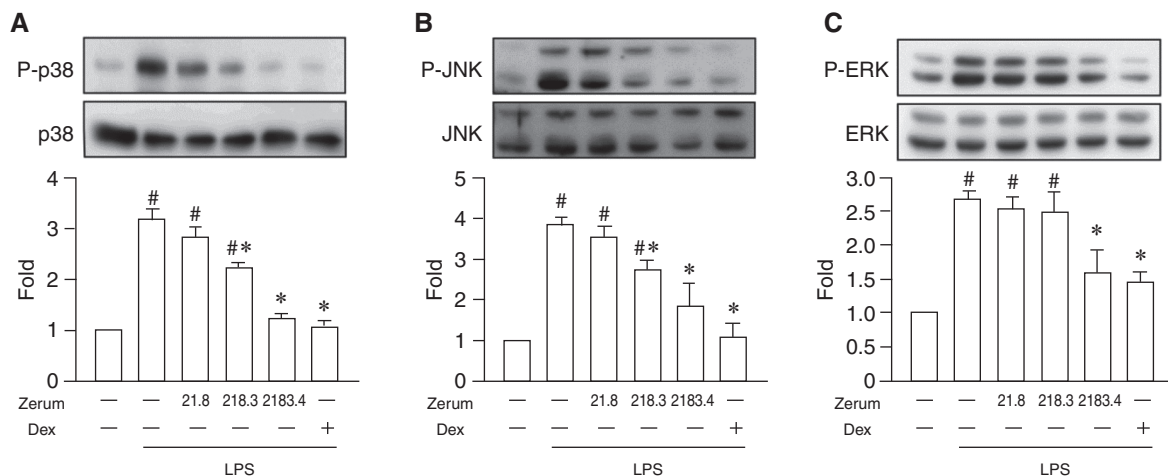

Fig. 6. Effect of zerumbone on LPS-induced phosphorylation of p38 MAPK, JNK, and ERK in lungs. Lung tissues harvested from post-treated mice were analyzed by Western blotting. The fold of p38 MAPK (A), JNK (B), and ERK (C) phosphorylation between the treated and control groups were calculated. Values are expressed as mean ± SD (n = 3 in each group). # represents a significant difference between the indicated and normal control group, and * represents a significant difference between the indicated and LPS treated groups, $P < 0.05$.

capacity, and results in hypoxemia and hypercapnia (13). At present study, we found that hypoxemia and hypercapnia were both induced by LPS in ALI mouse model. LPS-induced hypoxemia and hyper-

capnia were attenuated by zerumbone. Our previous study has shown that histopathological changes and lung edema can be reduced by zerumbone in LPS-induced ALI mice (18). Based on these results, we

had at present conclusive evidence which indicated LPS-induced ALI is prevented by zerumbone *via* reversed blood gas exchange *in vivo*.

Neutrophils, also called polymorphonuclear leukocytes or neutrophilic granulocytes, play a crucial role in the first line of innate immunity. Neutrophils are the most numerous leukocytes in circulation and participate in resisting against various bacterial and fungal infections. However, improper activation of neutrophils can lead to tissue damage in the process of exaggerating inflammatory reaction (17). At present, neutrophils infiltration into alveolar space induced by LPS appeared to be the same in context as described in previous studies (18, 37). We found that zerumbone reduced the content of neutrophils in BALF of LPS-induced ALI mice. Neutrophil infiltration into the air ways is due to the disruption of vascular endothelial barrier integrity, which increases vascular permeability and results in plasma leakage. In diabetic rats, retinal vascular permeability is reduced by zerumbone (19). At present study, the upregulation of protein concentration level in BALF was inhibited by zerumbone in ALI mice. These results indicated that zerumbone was able to attenuate LPS-induced ALI in mice *via* decreasing vascular endothelial barrier damage and neutrophils infiltration.

Neutrophils are the earliest phagocytes to migrate into the infective or inflammatory sites. In the process of neutrophils migration, expression of adhesion molecules such as immunoglobulin (Ig) superfamily and its ligands, integrins, are very important surface markers for neutrophils and vascular endothelial cells in inflammation respectively (20). Constitutive expression of ICAM-1 and VCAM-1 on vascular endothelial cells stimulated by LPS can interact with lymphocyte function associated (LFA-1), integrin alpha M (Mac-1), and very late antigen-4 (VLA-4) on neutrophils. These interactions of Ig superfamily-integrins promote neutrophil-endothelial cell adhesion, sticking, and transmigration (7, 27). In streptozotocin (STZ)-induced diabetic rats, the mRNA and protein expression of ICAM-1 and VCAM-1 is reduced by zerumbone in retina and renal tissues (30, 31). In addition, expression of ICAM-1 mRNA is reduced by zerumbone in the pancreatic tissue of acute necrotizing pancreatitis and hepatic tissue of pancreatitis-induced hepatic injury (34). At present, we also found similar results. Pretreatment with zerumbone at 218.3 μg/kg significantly inhibited ICAM-1 expression in BALF of mice with LPS-induced ALI. However, the level of VCAM-1 expression was only slightly inhibited by zerumbone even at 2183.4 μg/kg. These results suggested that in mice with LPS-induced ALI, zerumbone reduced neutrophils infiltration *via* decreasing the expression of ICAM-1.

Proinflammatory cytokines IL-1β and MIP-2 enhance the expression of adhesion molecules and neutrophils infiltration in ALI (8). Zerumbone significantly reduced the expression of IL-1β in the pancreatic tissue of acute necrotizing pancreatitis, hepatic tissue of pancreatitis-induced hepatic injury, retina, and renal tissues of STZ-induced ALI in murine model (30, 31, 34). Same as reported in previous studies, IL-1β expression was reduced by zerumbone in LPS-induced ALI mice. Moreover, we found LPS-induced generation of MIP-2 was reduced by zerumbone in a concentration-dependent manner. These results indicated that the prevention of LPS-induced adhesion molecules expression by zerumbone was due to reduction of IL-1β and MIP-2 expressions.

NF-κB, which serves as a critical proinflammatory transcription factor for regulating immune and proinflammatory responses, modulates the transcription of multiple proinflammatory mediators including IL-1β, MIP-2, ICAM-1, and VCAM-1 in ALI mice (37, 36). In resting state, NF-κB is associated with IκB and maintained in an inactivated state in cytoplasm. Phosphorylation of IκB, induced by IκB kinase, leads to IκB degradation and results in NF-κB activation. In murine model of ultraviolet B-induced photokeratitis, activation and translocation of NF-κB are inhibited by zerumbone in cornea (3). Expression of scavenger receptor genes is attenuated by zerumbone *via* NF-κB activation in tetradecanoylphorbol-13-acetate-stimulated THP-1 human monocytic cells (6). In our laboratory, we also found the activation of NF-κB is reduced by zerumbone in LPS-induced ALI mice (10). For the present, it may be useful to study more of the important features in NF-κB activation, such as NF-κB phosphorylation and IκB degradation. In the present study, western blot assay showed that the NF-κB phosphorylation and IκB degradation inhibited by various concentrations of zerumbone were in direct correlation with the generation of proinflammatory mediators induced by LPS. These results indicated that the expression of proinflammatory mediators reduced by zerumbone was due to inhibition of NF-κB activation *via* NF-κB phosphorylation and IκB degradation.

MAPK family, including p38 MAPK, ERK, and JNK, participates in IκB degradation and proinflammatory responses in LPS-induced ALI (34). Phosphorylation of p38 MAPK and JNK can be stimulated by LPS to activate the proinflammatory response in ALI mice and RAW264.7 macrophages (29, 39). Meanwhile, phosphorylation of p38 MAPK, ERK, and JNK were induced by LPS in ALI mice in present study which is in accordance
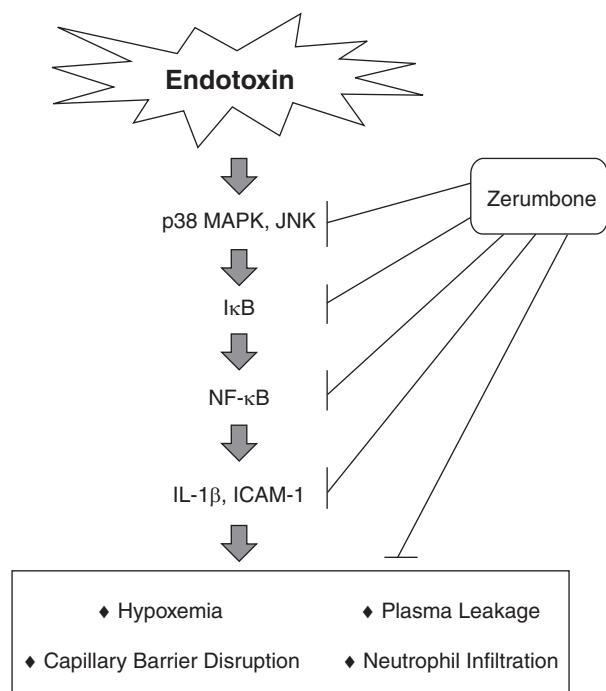
Fig. 7. Schemes of the protective effect of zerumbone on LPS-induced ICAM-1 and cytokines expression *via* p38 MAPK/JNK- IκB/NF-κB pathway in mouse model of ALI.

with previous study (16). Pretreatment with zerumbone at 218.3 μg/kg and up significantly inhibited phosphorylation of p38 MAPK and JNK in a concentration-dependent manner in LPS-induced ALI mice. However, the level of ERK1/2 phosphorylation was slightly inhibited in these mice when the concentration of zerumbone was up to 2183.4 μg/kg. The parallel trends between phosphorylation of NF-κB, degradation of IκB, and phosphorylation of p38 MAPK and JNK were inhibited by zerumbone. Therefore, the reduction of phosphorylation of NF-κB and degradation of IκB by zerumbone was partially due to its inhibitory effect on the production of p38 MAPK and JNK phosphorylation.

Our laboratory has purposed that production of IL-6 and TNFα, expression of inducible nitric oxide synthase and cyclooxygenase-2, and leukocytes infiltration into alveolar space can be reduced by zerumbone *via* Akt-NF-κB activation in LPS-induced ALI mice model (10). In addition, pretreatment with zerumbone can reduce histopathlgical changes, activation of myeloperoxidase (MPO) and metallopeptidase-9 (MMP-9), and lipid peroxidation occur in lungs in LPS-induced ALI mice *via* upregulation of antioxidative enzymes activation and nuclear factor erythroid 2-related factor (Nrf2)-heme oxygenase (HO-1) pathway (18). At present, as shown

in Fig. 7, we demonstrated that zerumbone significantly ameliorated the arterial blood gas exchanges, neutrophils infiltration, and increased pulmonary vascular permeability in the mouse model of LPS-induced ALI. The molecular mechanisms involved in the protective effect of zerumbone were (a) decreased expression of adhesion molecules including ICAM-1, (b) decreased expression of proinflammatory cytokines such as IL-1β and MIP-2, (c) decreased IκB degradation and NF-κB phosphorylation, and (d) downregulation of p38 MAPK and JNK phosphorylation. These results suggested the possibility of zerumbone as a protective compound for ALI associated with infection caused by LPS *via* the mechanisms including downregulation of Akt, p38 MAPK/JNK, and IκB/NF-κB pathways and upregulation of antioxidative enzymes activation and Nrf2-HO-1 pathways.

Acknowledgments

Conflicts of Interest

The authors declare no conflict of interest.

References

1. Abdul, A.B., Abdelwahab, S.I., Al-Zubairi, A.S., Elhassan, M.M. and Murali, S.M. Anticancer and antimicrobial activities of zerumbone from the Rhizomes of *Zingiber zerumbut*. *Int. J. Pharmacol*. 4: 301-304, 2008.
2. Chaung, H.C., Ho, C.T. and Huang, T.C. Anti-hypersensitive and anti-inflammatory activities of water extract of *Zingiber zerumbet* (L.) Smith. *Food Agric. Immunol*. 19: 117-129, 2008.
3. Chen, B.Y., Lin, D.P., Wu, C.Y., Teng, M.C., Sun, C.Y., Tsai, Y.T., Su, K.C., Wang, S.R. and Chang, H.H. Dietary zerumbone prevents mouse cornea from UVB-induced photokeratitis through inhibition of NF-κB, iNOS, and TNF-α expression and reduction of MDA accumulation. *Mol. Vis*. 17: 854-863, 2011.
4. Chen, W.Y., Huang, Y.C., Yang, M.L., Lee, C.Y., Chen, C.J., Yeh, C.H., Pan, P.H., Horng, C.T., Kuo, W.H. and Kuan, Y.H. Protective effect of rutin on LPS-induced acute lung injury *via* downregulation of MIP-2 expression and MMP-9 activation through inhibition of Akt phosphorylation. *Int. Immunopharmacol*. 22: 409-413, 2014.
5. Chen, X., Yang, X., Liu, T., Guan, M., Feng, X., Dong, W., Chu, X., Liu, J., Tian, X., Ci, X., Li, H., Wei, J., Deng, Y., Deng, X., Chi, G. and Sun, Z. Kaempferol regulates MAPKs and NF-kappaB signaling pathways to attenuate LPS-induced acute lung injury in mice Int. *Immunopharmacol*. 14: 209-216, 2012.
6. Eguchi, A., Kaneko, Y., Murakami, A. and Ohigashi, H. Zerum-

bone suppresses phorbol ester-induced expression of multiple scavenger receptor genes in THP-1 human monocytic cells. *Biosci. Biotechnol. Biochem*. 71: 935-945, 2007.

7. Etzioni, A. Adhesion molecules-their role in health and disease. *Nature* 39: 191-198, 1996.

8. Grommes, J. and Soehnlein, O. Contribution of neutrophils to acute lung injury. *Mol. Med*. 17: 293-307, 2011.

9. Hammer, J. Acute lung injury: pathophysiology, assessment and current therapy. *Paediatric. Respir. Rev*. 2: 10-21, 2001.

10. Ho, Y.C., Lee, S.S., Yang, M.L., Huang-Liu, R., Lee, C.Y., Li, Y.C. and Kuan, Y.H. Zerumbone reduced the inflammatory response of acute lung injury in endotoxin-treated mice *via* Akt-NFκB pathway. *Chem. Biol. Interact*. 271: 9-14, 2017.

11. Huang, Y.C., Horng, C.T., Chen, S.T., Lee, S.S., Yang, M.L., Lee, C.Y., Kuo, W.H., Yeh, C.H. and Kuan, Y.H. Rutin improves endotoxin-induced acute lung injury *via* inhibition of iNOS and VCAM-1 expression. *Environ. Toxicol*. 31: 185-191, 2016.

12. Imam, F., Al-Harbi, N.O., Al-Harbi, M.M., Ansari, M.A., Zoheir, K.M., Iqbal, M., Anwer, M.K., Al Hoshani, A.R., Attia, S.M. and Ahmad, S.F. Diosmin downregulates the expression of T cell receptors, pro-inflammatory cytokines and NF-κB activation against LPS-induced acute lung injury in mice. *Pharmacol. Res*. 102: 1-11, 2015.

13. Johnson, E.R. and Matthay, M.A. Acute lung injury: epidemiology, pathogenesis, and treatment. *J. Aerosol. Med. Pulm. Drug Deliv*. 23: 243-252, 2010.

14. Kader, G., Nikkon, F., Rashid, M.A. and Yeasmin, T. Antimicrobial activities of the rhizome extract of *Zingiber zerumbet* Linn. *Asian Pac. J. Trop. Biomed*. 1: 409-412, 2011.

15. Kitayama, T., Nagao, R., Masuda, T., Hill, R.K., Morita, M., Takatani, M., Sawada, S. and Okamoto, T. The chemistry of zerumbone IV: asymmetric synthesis of Zerumbol. *J. Mol. Catal. B Enzym*. 17: 75-79, 2002.

16. Lee, C.Y., Yang, J.J., Lee, S.S., Chen, C.J., Huang, Y.C., Huang, K.H. and Kuan, Y.H. Protective effect of Ginkgo biloba leaves extract, EGb761, on endotoxin-induced acute lung injury *via* a JNK- and Akt-dependent NFκB pathway. *J. Agric. Food Chem*. 62: 6337-6344, 2014.

17. Leliefeld, P.H., Wessels, C.M., Leenen, L.P., Koenderman, L. and Pillay, J. The role of neutrophils in immune dysfunction during severe inflammation. *Crit. Care* 20: 73, 2016.

18. Leung, W.S., Yang, M.L., Lee, S.S., Kuo, C.W., Ho, Y.C., Huang-Liu, R., Lin, H.W. and Kuan, Y.H. Protective effect of zerumbone reduces lipopolysaccharide-induced acute lung injury *via* antioxidative enzymes and Nrf2/HO-1 pathway. *Int. Immunopharmacol*. 46: 194-200, 2017.

19. Liu, W.Y., Tzeng, T.F. and Liu, I.M. Zerumbone, a bioactive sesquiterpene, ameliorates diabetes-induced retinal microvascular damage through inhibition of phospho-p38 mitogen-activated protein kinase and nuclear factor-κB pathways. *Molecules* 21: 1708, 2016.

20. Meziani, F., Delabranche, X., Asfar, P. and Toti, F. Bench-to-bedside review: circulating microparticles--a new player in sepsis? *Crit. Care* 14: 236, 2010.

21. Mokra, D. and Kosutova, P. Biomarkers in acute lung injury. *Front. Pediatr*. 209: 52-58, 2015.

22. Nag, A., Bandyopadhyay, M. and Mukherjee, A. Antioxidant activities and cytotoxicity of *Zingiber zerumbet* (L.) Smith rhizome. *J. Pharmacogn. Phytochem*. 2: 102-108, 2013.

23. Rubenfeld, G.D., Caldwell, E., Peabody, E., Weaver, J., Martin, D.P., Neff, M., Stern, E.J. and Hudson, L.D. Incidence and outcomes of acute lung injury. *N. Engl. J. Med*. 20: 1685-1693, 2005.

24. Santosh Kumar, S.C., Srinivas, P., Negi, P.S. and Bettadaiah, B.K. Antibacterial and antimutagenic activities of novel zerumbone analogues. *Food Chem*. 141: 1097-1103, 2013.

25. Sidahmed, H.M., Hashim, N.M., Abdulla, M.A., Ali, H.M., Mohan, S., Abdelwahab, S.I., Taha, M.M., Fai, L.M. and Vadivelu, J. Antisecretory, gastroprotective, antioxidant and anti-Helicobcter pylori activity of zerumbone from *Zingiber zerumbet* (L.) Smith. *PLoS One* 10: e88, 2015.

26. Sperandeo, P., Martorana, A.M. and Polissi, A. Lipopolysaccharide biogenesis and transport at the outer membrane of Gram-negative bacteria. *Biochim. Biophys. Acta* 16: 30274-30278, 2016.

27. Stadtmann, A. and Zarbock, A. The role of kindlin in neutrophil recruitment to inflammatory sites. *Curr. Opin. Hematol*. 24: 38-45, 2017.

28. Sulaiman, M.R., Perimal, E.K., Akhtar, M.N., Mohamad, A.S., Khalid, M.H., Tasrip, N.A., Mokhtar, F., Zakaria, Z.A., Lajis, N.H. and Israf, D.A. Anti-inflammatory effect of zerumbone on acute and chronic inflammation models in mice. *Fitoterapia* 81: 855-858, 2010.

29. Sung, M.J., Davaatseren, M., Kim, S.H., Kim, M.J. and Hwang, J.T. Boehmeria nivea attenuates LPS-induced inflammatory markers by inhibiting p38 and JNK phosphorylations in RAW264.7 macrophages. *Pharm. Biol*. 51: 1131-1136, 2013.

30. Tzeng, T.F., Liou, S.S., Chang, C.J. and Liu, I.M. Zerumbone, a tropical ginger sesquiterpene, ameliorates streptozotocin-induced diabetic nephropathy in rats by reducing the hyperglycemia-induced inflammatory response. *Nutr. Metab. (Lond.)* 10: 64, 2013.

31. Tzeng, T.F., Liou, S.S., Tzeng, Y.C. and Liu, I.M. Zerumbone, a phytochemical of Subtropical Ginger, protects against hyperglycemia-induced retinal damage in experimental diabetic rats. *Nutrients* 8: E449, 2016.

32. Wang, C. Obesity, inflammation, and lung injury (oili): the good. *Mediat. Inflamm*. 2014: 978463, 2014.

33. Wei, C.Y., Sun, H.L., Yang, M.L., Yang, C.P., Chen, L.Y., Li, Y.C., Lee, C.Y. and Kuan, Y.H. Protective effect of wogonin on endotoxin-induced acute lung injury *via* reduction of p38 MAPK and JNK phosphorylation. *Environ. Toxicol*. 32: 397-403, 2017.

34. Wenhong, D., Jia, Y., Weixing, W., Xiaoyan, C., Chen, C., Sheng, X. and Hao, J. Zerumbone attenuates the severity of acute necrotizing pancreatitis and pancreatitis-induced hepatic injury. *Mediators Inflamm*. 2012: 156507, 2012.

35. Wheeler, A.P. and Bernard, G.R. Acute lung injury and the acute respiratory distress syndrome: A clinical review. *Lancet* 369: 1553-1564, 2007.

36. Yeh, C.H., Yang, J.J., Yang, M.L., Li, Y.C. and Kuan, Y.H. Rutin decreases lipopolysaccharide-induced acute lung injury *via* inhibition of oxidative stress and the MAPK-NF-κB pathway. *Free Radic. Biol. Med*. 69: 249-257, 2014.

37. Yeh, Y.C., Yang, C.P., Lee, S.S., Horng, C.T., Chen, H.Y., Cho, T.H., Yang, M.L., Lee, C.Y., Li, M.C. and Kuan, Y.H. Acute lung injury induced by lipopolysaccharide is inhibited by wogonin in mice *via* reduction of Akt phosphorylation and RhoA activation. *J. Pharm. Pharmacol*. 68: 257-263, 2016.

38. Yob, N.J., Jofrry, S.M., Affandi, M.M., The, L.K., Salleh, M.Z. and Zakaria, Z.A. *Zingiber zerumbet* (L.) Smith: a review of its ethnomedicinal, chemical, and pharmacological uses. *Evid. Based Complement. Alternat. Med*. 2011: 543216, 2011.

39. Yu, X., Yu, S., Chen, L., Liu, H., Zhang, J., Ge, H., Zhang, Y., Yu, B. and Kou, J. Tetrahydroberberrubine attenuates lipopolysaccharide-induced acute lung injury by down-regulating MAPK, AKT, and NF-κB signaling pathways. *Biomed. Pharmacother*. 82: 489-497, 2016.